molecules

IMPACT FACTOR 4.6

Indexed in: PubMed

CITESCORE 6.7

Article

Microfluidic Diffusion Sizing Applied to the Study of Natural Products and Extracts That Modulate the SARS-CoV-2 Spike RBD/ACE2 Interaction

Jason Fauquet, Julie Carette, Pierre Duez, Jiuliang Zhang and Amandine Nachtergael

Special Issue

Natural Compounds for Disease and Health II

Edited by

Dr. George P.H. Leung and Dr. Jingjing Li

MDPI

https://doi.org/10.3390/molecules28248072

molecules

MDPI

Article

Microfluidic Diffusion Sizing Applied to the Study of Natural Products and Extracts That Modulate the SARS-CoV-2 Spike RBD/ACE2 Interaction

Jason Fauquet [1,†], Julie Carette [1,*,†], Pierre Duez [1], Jiuliang Zhang [2] and Amandine Nachtergael [1]

[1] Unit of Therapeutic Chemistry and Pharmacognosy, University of Mons (UMONS), 7000 Mons, Belgium; jason.fauquet@umons.ac.be (J.F.); pierre.duez@umons.ac.be (P.D.); amandine.nachtergael@umons.ac.be (A.N.)
[2] College of Food Science and Technology, Huazhong Agricultural University, Wuhan 430070, China; zjl_ljz@mail.hzau.edu.cn
* Correspondence: julie.carette@umons.ac.be
† These authors contributed equally to this work.

Abstract: The interaction between SARS-CoV-2 spike RBD and ACE2 proteins is a crucial step for host cell infection by the virus. Without it, the entire virion entrance mechanism is compromised. The aim of this study was to evaluate the capacity of various natural product classes, including flavonoids, anthraquinones, saponins, ivermectin, chloroquine, and erythromycin, to modulate this interaction. To accomplish this, we applied a recently developed a microfluidic diffusional sizing (MDS) technique that allows us to probe protein-protein interactions via measurements of the hydrodynamic radius (R_h) and dissociation constant (K_D); the evolution of R_h is monitored in the presence of increasing concentrations of the partner protein (ACE2); and the K_D is determined through a binding curve experimental design. In a second time, with the protein partners present in equimolar amounts, the R_h of the protein complex was measured in the presence of different natural products. Five of the nine natural products/extracts tested were found to modulate the formation of the protein complex. A methanol extract of *Chenopodium quinoa* Willd bitter seed husks (50 µg/mL; bisdesmoside saponins) and the flavonoid naringenin (1 µM) were particularly effective. This rapid selection of effective modulators will allow us to better understand agents that may prevent SARS-CoV-2 infection.

Keywords: hydrodynamic radius; dissociation constant; protein-protein interaction

Citation: Fauquet, J.; Carette, J.; Duez, P.; Zhang, J.; Nachtergael, A. Microfluidic Diffusion Sizing Applied to the Study of Natural Products and Extracts That Modulate the SARS-CoV-2 Spike RBD/ACE2 Interaction. *Molecules* **2023**, *28*, 8072. https://doi.org/10.3390/molecules28248072

Academic Editors: George P.H. Leung and Jingjing Li

Received: 30 October 2023
Revised: 29 November 2023
Accepted: 11 December 2023
Published: 13 December 2023

1. Introduction

It is difficult to ignore the global health crisis caused by severe acute respiratory syndrome coronavirus 2 (SARS-CoV-2). First appearing in Wuhan, China, in December 2019, this single-stranded positive sense RNA virus led to an estimated 771 million infections and 6.9 million deaths [1]. Currently, although it has attenuated, the 2019 coronavirus disease (COVID-19) pandemic continues worldwide, with many variants arising. Thus, the need to minimize the spread of the virus and to find rapid and effective prevention and treatment means has pushed scientists to expand their knowledge about the disease considerably.

Even though the methods of transmission are multiple, the major means of dispersion are still through the respiratory tract [2,3]. The key factor for viral invasion in humans relies on an interaction between the receptor binding domain (RBD) of the spike protein (S protein) and human angiotensin-converting enzyme 2 (ACE2); this interaction initiates membrane fusion, allowing virus entry, and it is involved in syncytia formation, potentially implicated in viral dissemination and the immune response [4–6].

The well-known "crown-like" appearance from which the family name was inspired seems to belong to the presence of two conformations of "spike" proteins on the surface of mature virion. The "prefusion" conformation is first produced as a trimerized precursor composed of three protomers [7], each protomer being composed of two subunits: the

S1 carrying the RBD domain mainly involved in the interaction with the ACE2 receptor; and the S2 anchoring the proteins into the membrane. The RBD domain standing at the apex of each protomer adopts two distinct "prefusion" conformations, called "up" if the receptor is accessible and "down" if it is not [8]. This position varies from one prefusion S protein to another, adopting, for example, one RBD "up" and two "down". Inducing the fusion process requires protein S cleavage, leading to a new conformation, "postfusion", consisting of a loss of S1 subunits and refolding of S2 subunits. This new conformation also appears in the absence of interaction with ACE2, which explains the presence of these two conformations at the surface of the mature virion [7,9–11].

ACE2, the human-functional receptor for SARS-CoV-2, has several roles, ranging from enzymatic activities with various substrates to amino acid transporter partners, but its main function is to degrade angiotensin II into angiotensin 1–7 [8,12], playing a key role in maintaining salt and water homeostasis. ACE2 is distributed in the lungs, cardiovascular system, gut, kidneys, central nervous system, and adipose tissue. However, the highest ACE2 concentrations are found in the lungs, in which 83% of the cells expressing ACE2 are type 2 alveolar cells of the pulmonary epithelium [13,14]. The ACE2 protein is composed of 805 amino acids and has two functional parts, an N-terminal domain containing a peptidase M2 function and a C-terminal collectrin domain; the human ACE2 peptidase domain interacts with the RBD of the viral spike protein. This interaction leads to a conformational change in the S-protein, allowing for fusion with the host cell membrane. This binding ACE2-RBD has been shown to be a relevant target to prevent infection [15]. In the present paper, we applied a promising method based on microfluidic diffusional sizing (MDS) to highlight several compounds able to modulate and disrupt this interaction [16].

The MDS method, initially introduced in 2016 [17], has garnered over 111 citations, indicating its swift emergence as a versatile technique, notably for the identification and quantification of protein-protein interactions in various mixtures. The versatility of MDS positions it for a broad spectrum of applications, including the analysis of lipids, proteins, nucleic acids, and proteins, the sizing of single molecules, and the monitoring of biomolecule assembly, for example, antigen to antibody or protein to chaperone.

Natural products provide original and diversified insights to develop a therapeutic arsenal against viral infections, notably COVID-19; indeed, they offer a remarkable heterogeneity of chemical structures capable of targeting different stages of the SARS-CoV-2 life cycle [18–20]. Several classes of natural products have notably been considered to modulate the spike RBD/ACE2 interaction. Among them, some deserve further research, as they could do the following:

- ✓ Show interesting binding energy to one or both protein partners (flavonoids [18,21–27], terpenoids [28–34], macrocycles [5,35–38], alkaloids [28], and anthraquinones [32,39,40]).
- ✓ Disrupt the spike RBD/ACE2 complex, bind the spike protein, or inhibit ACE2 activity (polyphenols such as flavonoids [23,24,41], stilbenes [42,43] or tannins [44,45]; terpenoids [46,47], and anthraquinones [48]).
- ✓ Prevent viral entry into cells expressing ACE2 (flavonoids [49], cannabinoids [50], terpenoids [51,52], quinones [53], macrocycles [54], alkaloids [55,56], and anthraquinones [57]).

These previous data served as the basis for the selection of the varied structures studied in the present work for their impact on spike RBD/ACE2 binding, i.e., flavonoids, anthraquinones, saponins, ivermectin, chloroquine, and erythromycin.

2. Results

2.1. SARS-CoV-2 Spike RBD/ACE2 Binding: Determination of K_D

The dissociation constant (K_D) of the SARS-CoV-2 spike RBD/ACE2 complex was measured over a range of ACE2 concentrations (180 pM to 750 nM) for a spike RBD concentration set at 20 nM; these concentrations were selected to yield two distinct plateaus. The $R_{h\ values}$ measured for free spike RBD and the spike RBD/ACE2 complex at saturation are 2.97 nm (95% confidence interval, 2.90–3.05 nm) and 4.35 nm (95% confidence interval,

4.21–4.50 nm), respectively. Fitting of the obtained sigmoid curve (Figure 1) yielded a K_D of 24.2 nM (95% confidence interval, 10.6–48.9 nM). The obtained K_D is within the range of the previously published K_D (Table 1).

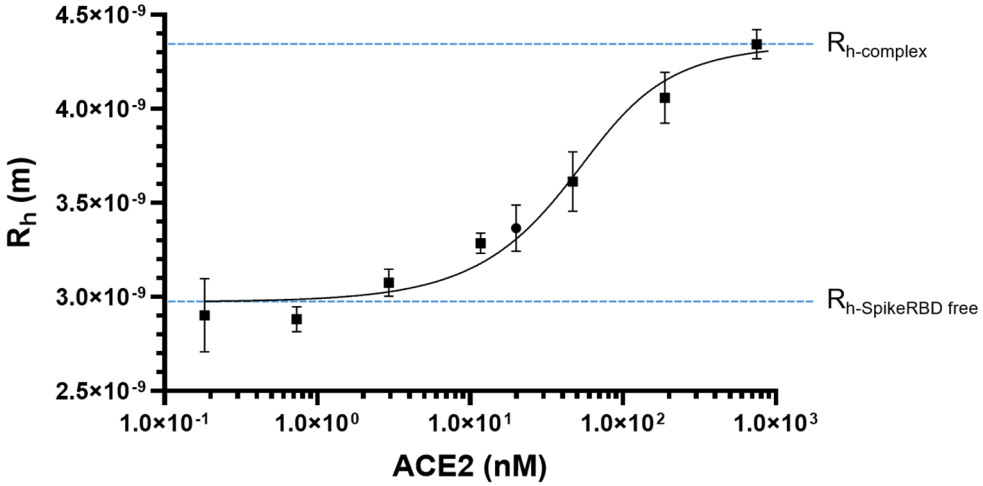

Figure 1. Microfluidic diffusional sizing determination of K_D for the spike RBD (20 nM)/ACE2 complex (DMSO, 1% *v*/*v*; room t°). R_h as a function of ACE2 concentration. ACE2, 180 pM to 750 nM; spike RBD, 20 nM; mean ± standard deviation (n = 4).

Table 1. Interaction between ACE2 and SARS-CoV-2 RBD or SARS-CoV-2 spike. Published KD as measured by surface plasmon resonance (SPR) or biolayer interferometry (BLI).

Ligand-Receptor	K_D Determination Method	K_D (nM)	Reference
SARS-CoV-2 RBD/ACE2	SPR	4.7	[58]
	SPR	63.0	[59]
	SPR	24.1	[24]
	SPR	17.0	[60]
	SPR	5.8	[61]
	SPR	44.2	[62]
	BLI	75.1	[63]
	BLI	161	[64]
	BLI	172	[44]
SARS-CoV-2 Spike/ACE2	SPR	14.7	[65]
	SPR	29.1	[66]
	SPR	76	[67]
	BLI	12.8	[68]
	BLI	1.2	[69]
	BLI	133.0	[70]

2.2. Validation of MDS Measurements

Given the relative recentness of the MDS method, a series of validation parameters were assessed, including selectivity, within- and between-chip reproducibility, accuracy, and precision.

The microdiffusion chips were proposed as single-use chips, and their eventual reuse was tested but found to be unreliable (Tables S1 and S2; Figure S2) as repeated measurements do not agree, preventing the determination of a K_D over a single chip. The criteria of selectivity, accuracy, precision, and quality of adjustment were then determined by running a single injection per chip. A summary of the validation data is presented in Table 2, while full data are reported in the Supplementary Materials.

Table 2. Summary of the validation data.

Criterion	What Is Assessed?	Result	Full Data (Supplementary Materials)
Selectivity	Eventual fluorescence interferences	No	Figure S1
Between-chips reproducibility	1 chip for 1 R_h measurement (n = 6)	CV = 3.99%	Table S1
Within-chip reproducibility	1 chip for R_h measurement X times at the same concentration (n = 8)	CV = 31.4%	Table S2
Determination of K_D over a single chip	1 chip for 1 K_D determination (7 points) (n = 3)	Erroneous values	Figure S2
Quality of adjustment	Coefficient of determination (R^2)	0.854–0.963	Table S7
Accuracy of R_h for the Spike $RBD_{labelled}$	Comparison of experimental R_h with a value predicted from a range of protein standards with globular conformation	105.4 ± 5.7% (n = 13)	Point 3
Precision	R_h—Intraday precision (n = 4)	CV = 2.90%	Table S5
	R_h—Total precision (n = 6)	CV = 6.27%	Table S4
	K_D—Total precision (n = 5)	CV = 20.8%	Table S6

2.3. Modulation of SARS-CoV-2 Spike RBD/ACE2 Binding by Natural Compounds

First, a day-to-day variation was observed for the R_h of the SARS-CoV-2 spike RBD/ACE2 complex itself; this could be related to a difference in chip temperature that is unavoidable, given that the system is not temperature controlled and depends on the laboratory environmental conditions. Consequently, daily controls were measured for the SARS-CoV-2 spike RBD/ACE2 complex in the absence of natural products; all data obtained in the presence of natural products were then compared to their daily controls. To minimize the effect of an eventual temperature change during daily experiments, the controls and samples were randomly analyzed within the same day.

Table 3 presents the modulation of the $R_{h\text{-complex}}$ when proteins are incubated in the presence of natural products. Quercetin reduces the $R_{h\text{-complex}}$ of SARS-CoV-2 Spike RBD/ACE2 by 11% at a concentration of 150 µM, while naringenin has an impact on the $R_{h\text{-complex}}$ at a concentration of only 1 µM with a significant positive $R_{h\text{-complex}}$ variation of approximately 10%.

The literature data indicate promising in vitro activities for ivermectin. In our MDS model, ivermectin induces a significant increase in the $R_{h\text{-complex}}$ by approximately 12% at a concentration of 1 nM. This effect seems to be concentration-dependent over the tested range. The dry extract of Rhei radix is active at a concentration of 100 µg/mL with an $Rh_{\text{-complex}}$ decrease of approximately 14%. The saponin-rich extract of *Chenopodium quinoa* husks has shown the most interesting activity; a modulatory effect was already statistically significant at a concentration of 50 µg/mL with an increase in the $R_{h\text{-complex}}$ by approximately 40%. The observed effect appears dose-dependent, with an $R_{h\text{-complex}}$ increase of approximately 150% at a concentration of 200 µg/mL. Finally, natural products that were noneffective in our experimental design are summarized in Table 4.

Table 3. Natural products (NPs) effectively modulate the R_h of the SARS-CoV-2 spike RBD/ACE2 protein complex.

Natural Product (NP)	Quercetin		Naringenin		Ivermectin		Rhei Radix EtOH Dry Extract		*Chenopodium quinoa* Willd. MeOH Dry Extract (Husks)	
	Range Tested	**1st Effective Concentration**	**Range Tested**	**1st Effective Concentration**	**Range Tested**	**1st Effective Concentration**	**Range Tested**	**1st Effective Concentration**	**Range Tested**	**1st Effective Concentration**
	0.1–150 μM	**150 μM**	**0.1–50 μM**	**1 μM**	**1–100 nM**	**1 nM**	**1–100 μg/mL**	**100 μg/mL**	**1–200 μg/mL**	**50 μg/mL**
R_h of daily control (nm) (mean ± SD)	3.28 ± 0.12		2.91 ± 0.05		3.19 ± 0.07		3.03 ± 0.08		2.14 ± 0.02	
R_h in the presence of NP (nm) (mean ± SD)	3.35 ± 0.07 to 2.92 ± 0.03	2.92 ± 0.03	3.09 ± 0.05 to 3.21 ± 0.07	3.21 ± 0.07	3.57 ± 0.07 to 4.09 ± 0.08	3.57 ± 0.07	3.03 ± 0.07 to 2.61 ± 0.05	2.61 ± 0.05	2.34 ± 0.22 to 5.33 ± 0.31	3.0 ± 0.1
Direction of R_h variation	Decrease		Increase		Increase		Decrease		Increase	
R_h variation (%) (mean ± SD)	2.12 ± 0.09 to −11.09 ± 0.43	−11.09 ± 0.43	6.08 ± 0.15 to 19.01 ± 0.85	9.99 ± 0.29	11.78 ± 0.40 to 27.97 ± 0.82	11.78 ± 0.40	−0.15 ± 0.01 to −13.97 ± 0.46	−13.97 ± 0.46	9.19 ± 0.87 to 148.98 ± 8.76	39.92 ± 1.91

Daily control was the mix spike RBD (20 nM)/ACE2 (20 nM) analyzed on the same day as the concerned NP. The first effective concentration is the concentration yielding a significant difference from the R_h of the daily control (n = 3; one-way ANOVA with post hoc Student's *t* test, Bonferroni correction; $p < 0.05$).

Table 4. Natural products (NP) that do not modulate the R_h of the SARS-CoV-2 spike RBD/ACE2 protein complex.

Natural Product (NP)	Naringin	Chloroquine	Erythromycin	*Gingko biloba* L. Dry Extract (Leaves)
Range tested	0.1–50 µM	1–1000 µM	0.1–50 µM	1–200 µg/mL
R_h of daily control (nm) (mean ± SD)	3.31 ± 0.06	2.87 ± 0.04	3.14 ± 0.05	2.39 ± 0.11
R_h of NP (nm) (mean ± SD)	3.26 ± 3.38–3.46 ± 0.12	2.76 ± 0.13–2.94 ± 0.03	3.06 ± 0.07–3.11 ± 0.08	2.35 ± 0.03–2.34 ± 0.16
R_h variation (%) (mean ± SD)	−1.64 ± 0.03–4.5 ± 0.2	−3.92 ± 0.20–2.11 ± 0.03	−2.29 ± 0.06–−0.73 ± 0.02	−1.75 ± 0.08–−2.10 ± 0.17
p Value	>0.9999–0.1256	0.4134–>0.9999	0.8427–>0.9999	>0.9999–>0.9999

Daily control was the mix Spike RBD (20 nM)/ACE2 (20 nM) analyzed on the same day as the concerned NP. None of the tested concentrations yielded a significant difference from the R_h of the daily control (n = 3; one-way ANOVA with post hoc Student's *t* test, Bonferroni correction; $p > 0.05$).

3. Discussion

As shown in Figures 2 and 3, the binding between SARS-CoV-2 spike RBD and ACE2 could be modulated in two opposite ways by the tested natural compounds:

1. An increase in the hydrodynamic radius (higher $R_{h\text{-complex}}$) that could correspond either to a distension of the bound protein complex or to a clustering of natural compounds on the proteins; these should shift the affinity curve to the left and decrease K_D.
2. A decrease in the hydrodynamic radius (lower $R_{h\text{-complex}}$), possibly indicating a collapse or folding of the complex or a partial separation of the two protein partners; this should shift the affinity curve to the right and increase K_D.

Although it is difficult to define the impact of these modulations on virus entry, the MDS method has the advantage of quickly sorting natural compounds and extracts to pinpoint interfering phytochemicals that can then be evaluated in more detail.

3.1. Quercetin

The online *Traditional Chinese Medicine Systems Pharmacology (TCMSP) Database and Analysis Platform* (available at https://old.tcmsp-e.com/tcmsp.php; [71]; accessed on 30 October 2023) predicts quercetin as a potential key drug. Additionally, a molecular docking analysis by the software AutoDock 4.2 predicts binding energies of −7.92 kcal/mol to ACE2 and −8.41 kcal/mol to apike RBD [24]; such a value < −6.2 kcal/mol indicates a possible modulation of protein-protein binding [24,35,38,42,44,72].

The obtained results partly agree with the literature data; indeed, Pan et al. (2020), applying surface plasmon resonance, reported a strong modulation of the interaction, but at a much lower concentration of quercetin (12 µM). Although the concentration found effective here (>30 µM) may be toxic under physiological conditions [73], our results point to an interest in the research of molecules with related structures that would be active at low concentrations.

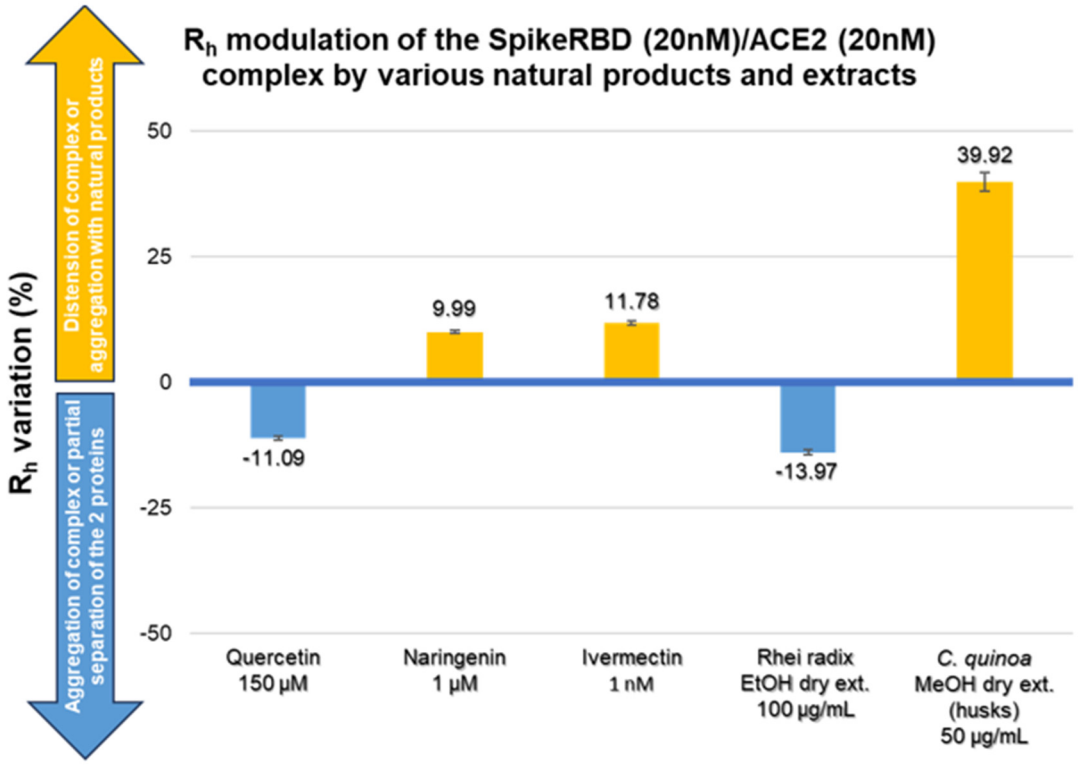

Figure 2. R_h modulation of the spike RBD (20 nM)/ACE2 (20 nM) complex by various natural products and extracts. R_h variation (%) of the spike RBD/ACE2 complex as a function of the tested natural products and extracts. Microfluidic diffusional size. Mean ± standard deviation. $n = 3$.

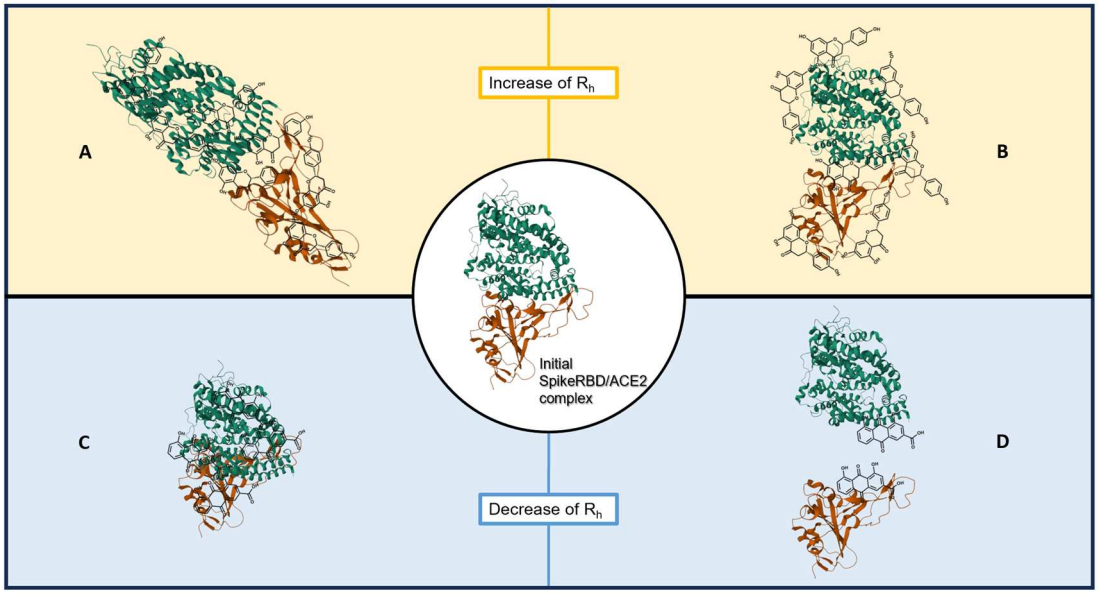

Figure 3. Schematic view of possible 3D conformational changes that the spike RBD/ACE2 complex could adopt in the presence of natural compounds, with their influence on R_h. The initial conformation of the spike RBD/ACE2 complex is represented in the center (PDB 6M0J); SARS-CoV-2 spike RBD is depicted in orange and ACE2 in green. (**A**) An increase in R_h could be due to distension of the complex; (**B**) An increase in R_h could be due to clustering of natural compounds on proteins; (**C**) A decrease in R_h could be due to collapse or folding of the complex; (**D**) A decrease in R_h could be due to (partial) separation of the 2 proteins.

3.2. Naringin and Naringenin

The flavanone naringenin, selected for its binding energy to ACE2 of −6.05 kcal/mol [27] and its ability to inhibit, in a dose-dependent manner, the entry of SARS-CoV-2 in Vero E6 cells [49], was found to be highly effective as a modulator of SARS-CoV-2 spike RBD/ACE2 binding (active at 1 µM). Concentrations of 15.7 µM (C_{Max}) could be achieved within 3.2 h after oral administration of 150 mg of naringenin (in 536 mg of *Citrus sinensis* extract); no adverse events or changes in blood markers were detected following the oral administration of a naringenin dose up to 900 mg [74].

In contrast, its heteroside, naringin, had no significant effect on the $R_{h\text{-}complex}$ despite its reported binding energy to ACE2 (−6.85 kcal/mol) [22]. This can probably be explained by steric hindrance of its O-rhamnoglucoside at position 7. Indeed, the predicted binding sites are significantly different for naringin (TYR-515, GLU-402, GLU-398, and ASN-394) and naringenin (PRO-146, LEU-143, and LYS-131) [22,27]; interestingly, our data indicate that the naringenin interaction site would be important for SARS-CoV-2 spike RBD/ACE2 binding.

3.3. Ivermectin

The literature data indicate promising in vitro activities for ivermectin; applied 2 h postinfection, ivermectin decreases the amount of viruses in infected Vero-hSLAM cells [54], while in silico modeling indicates ACE2 and spike RBD binding energies of −18 kcal/mol and −10.87 kcal/mol, respectively [37,38]. Despite this, a series of clinical studies did not yield conclusive data, except for the Biber et al. (2022) study, which showed a reduction in viral transmission in the frame of a clinical trial [75]. Our results are consistent with the in vitro data from the literature and place ivermectin on the side of interesting molecules that seem worthy of further investigation. Moreover, published data indicate that 23 to 27 nM (C_{Max}) could be achieved in plasma within 4.5 h after administration of a 6 mg tablet [76].

3.4. Rhei Radix

The dry extract of Rhei radix (*Rheum palmatum* L., *Rheum officinale* Baillon) was selected for its content in anthraquinones, notably rhein and emodin. Rhein has a predicted ACE2 binding energy of −8.73 kcal/mol [39], and emodin has binding energies to ACE2 and spike RBD of −7.26 kcal/mol and −8.8 kcal/mol, respectively [32,40]. Moreover, emodin has been reported to inhibit the entry of SARS-CoV-2 in Vero E6 cells [57]. Our first effective concentration corresponded to 3.6 µg/mL rhein, the only anthraquinone component of rhubarb that is absorbed into the blood in the human body [77]. In human volunteers, a single dose of rhubarb extract (50 mg/kg, corresponding to approximately 54 mg hydroxyanthracene derivatives, body weight 60 kg) [78] yielded a C_{Max} of 2.8 µg/mL within approximately 59 min. This indicates that the active concentration of hydroxyanthracene glycosides cannot be yielded in plasma and would rather favor a nasal administration of glycosides for a local preventive effect.

3.5. Bitter Chenopodium Quinoa Husks

Antiviral effects of some saponins have already been shown on different respiratory viruses, including the influenza virus, the human respiratory syncytial virus, and some coronaviruses [79]. For the latter, notably,

- In silico docking studies predict the following:
    1. Stigmastane-type steroidal saponins (vernonioside A2, vernonioside A4 and vernonioside D2) exhibit inhibitory potential against SARS-CoV-2 cysteine proteases [80].
    2. Saponins are potential inhibitors of the SARS-CoV-2 main protease (M^{pro}) with favorable ADMET profiles, with thirteen [81] and three (arjunic acid, thesapogenol B, euscaphic acid) [82] high potency compounds identified.

3. Glycyrrhizin has the potential to bind the host cell ACE2 receptor [83], and saikosaponin, glycyrrhizin, and ilexgenin A can bind both ACE2 and the SARS-CoV-2 main protease [84].
4. A series of saikosaponins favorably bind to the RDB region of the SARS-CoV-2 spike protein, with saikosaponin B4 as the best probable inhibitor [31], and saikosaponins bind to the NSP15 endoribonuclease and to the prefusion spike glycoprotein SARS-CoV-2, saikosaponins U and V, showing the highest affinity toward both proteins [33].

- In vitro studies indicate the following:
  1. Oleanane saikosaponin B2, at 6 μM, significantly inhibits viral attachment and penetration, impeding HCoV 229E infection in pre-, co-, and postinfection models [85].
  2. Glycyrrhizin at 600 μg/mL (EC50) inhibits the replication of 2 SARS-CoV clinical isolates in Vero cells [86] but was deemed inactive (EC50 > 400 μg/mL) when tested against 10 clinical strains of SARS-CoV in the fRhK4 cell line [87].
  3. Derivatives of glycyrrhizic acid are 10 to 70 times more active than glycyrrhizin itself in inhibiting the replication of a SARS-CoV clinical isolate in Vero cells; however, some compounds lose advantages in terms of viral selectivity [88].
  4. Aescin (6 μM) and four glycyrrhizin and aescin derivatives (<100 μM) showed activities toward SARS-CoV (H.K. strain) in Vero cells [89].

The dry methanolic extract of *C. quinoa* husk has a very high content of saponins, mostly bisdemosides (Figure 3); their structures are quite similar to those of the bisdesmosides saikosaponins U and V, which, in silico, present a high affinity toward the prefusion spike glycoprotein SARS-CoV-2 [33].

Regarding the first effective concentration (corresponding to 15 μg saponins/mL, expressed as hederacoside C), the poor intestinal absorption of saponins should be noted, which is mainly due to their unfavorable physicochemical traits (molecular mass, high hydrogen-bonding capacity, and high molecular flexibility) that underlie poor membrane permeability [90]. As the active concentration of bisdesmoside saponins will probably not be achievable in plasma, nasal administration should be favored for a local preventive effect.

3.6. Other Natural Products Tested

Chloroquine was selected because its in silico binding energy with the ACE2 protein was predicted to be −6.45 kcal/mol [28] and because of its inhibition of SARS-CoV-2 replication in Vero E6 cells [56]. Erythromycin was selected for its very high in silico affinity toward the SARS-CoV-2 spike RBD-His protein (−9 kcal/mol) [5].

Although several flavonoids have the ability to modulate protein-protein interactions [22,24,49,72], the dry extract of *Ginkgo biloba* L. leaves did not show any effect on the R_h of the studied protein complex even at high concentrations (200 μg/mL, corresponding to ~50 μg/mL flavonoids and 10.6 μg/mL terpene lactones, i.e., bilobalide and ginkgolides).

4. Materials and Methods

4.1. Tested Natural Products

A series of natural products were tested (Figure 4) for their capacity to modulate the spike RBD/ACE2 interaction, including 3 flavonoids (quercetin hydrate (≥95%, Sigma-Aldrich), Merck, Hoeilaart, Belgium); naringenin (≥98%, Carl Roth, Karlsruhe, Germany); naringenin rutinoside (naringin) (European Pharmacopoeia, EDQM, Strasbourg, France, CRS batch 1.0 id 004UT0)), ivermectin (88.2% B_{1a} and 2.1% B_{1b}, Sigma-Aldrich), chloroquine diphosphate (≥98%, Sigma-Aldrich), erythromycin (95.9%, Febelcare, Sint-Niklaas, Belgium), a dry ethanolic extract of Rhei radix (*Rheum palmatum* L., *Rheum officinale* Baillon; 5.69% hydroxyanthracene glycosides, expressed as rhein-8-glucoside, Conforma, Destelbergen, Belgium, batch 13D30/V54409), a reference dry extract of *Ginkgo biloba* L. leaves (European Pharmacopoeia, CRS Ginkgo dry extract for peak identification Y00010121; content in bilobalide, ginkgolide A, ginkgolide B, and ginkgolide C, 2.4%, 1.5%, 0.7%, and

0.7%, respectively; content in flavonoids, 22 to 27%), and a bitter seed husks. For the latter extract, 150 mg of *Chenopodium quinoa* Willd husks powder (0.5 mm) and 5 glass marbles (1 mm diameter) were mixed with 3.0 g of methanol 99% in a Mixer mill 400 (Retsch, Haan, Germany) (30 Hz, 10 min) and centrifuged (4000× *g*, 40 min, RT). The supernatant was evaporated to dryness under low pressure using a rotary evaporator (50 °C, 80 rpm) [91].

Each product or extract was dissolved in anhydrous dimethyl sulfoxide (DMSO-Thermo Fisher Scientific, Dilbeek, Belgium) and diluted as needed with phosphate-buffered saline at pH 7.4 without calcium, magnesium, and phenol red (PBS; 10010023-Thermo Fisher Scientific).

To the best of our knowledge, no drug targeting the spike RBD/ACE2 interaction is currently used in the clinic [92]. While the widely cited chloroquine, hydroxychloroquine, and ivermectin appeared somewhat deceiving in clinical trials, the potential of spike RBD/ACE2 modulators is such [93] that it remains worthwhile to define possibly useful compounds. Ivermectin is included in our tested natural products and can be considered a "reference drug".

4.2. Proteins and Fluorescence Labeling

All manipulations involving labeled proteins were protected from actinic light.

The original strain-His-tagged RBD protein and the soluble ACE2-Fc fusion protein were obtained from InvivoGen (Toulouse, France).

The RBD protein was reconstituted with PBS at a concentration of 333.3 µg/mL, added to Alexa Fluor 647 NHS ester (Thermo Fisher Scientific) at a dye-to-protein molar ratio of 3:1 and incubated at 4 °C overnight. The free dye was removed using the Antibody Conjugate Purification Kit (Thermo Fisher) following the manufacturer's instructions. The labeled purified protein was stored at −80 °C in PBS pH 7.4 containing 10% (*v*/*v*) glycerol for a maximum of 3 months.

4.3. SARS-CoV-2 Spike RBD/ACE2 Affinity Measurement by Microfluidic Diffusional Sizing

The binding between ACE2 and spike RBD proteins (affinity) was measured from the value of the equilibrium dissociation constants (K_D), obtained through a Fluidity ONE-W platform based on microfluidic diffusional sizing (MDS) and recently developed by Fluidic Analytics (Cambridge, UK) [17]. As shown in Figure 5, this method relies on microchips traveled by 2 laminar flows, parallel to each other and in direct contact, each flow leading to a fluorescence detector; the labeled species and the unlabeled (potential) partner are injected in the first flow, while the second flow is composed of a blank buffer. Due to a simple diffusion mechanism, species migrate from one flow to the second, depending on their hydrodynamic radii. The ratio of fluorescence intensities measured in each flow allows us to determine the diffusional coefficient D (m^2/s) through a proprietary equation [99]; the Stokes–Einstein equation establishes the relationship between D and the hydrodynamic radius R_h:

$$D = \frac{kT}{f} = \frac{kT}{6\pi\eta R_h},$$

where D is the diffusional coefficient (m^2/s); k is the Boltzman constant; T is the temperature (K); η is the viscosity (Pa × s); f is the fractional coefficient for a solid sphere in a viscous medium; and R_h is the hydrodynamic radius.

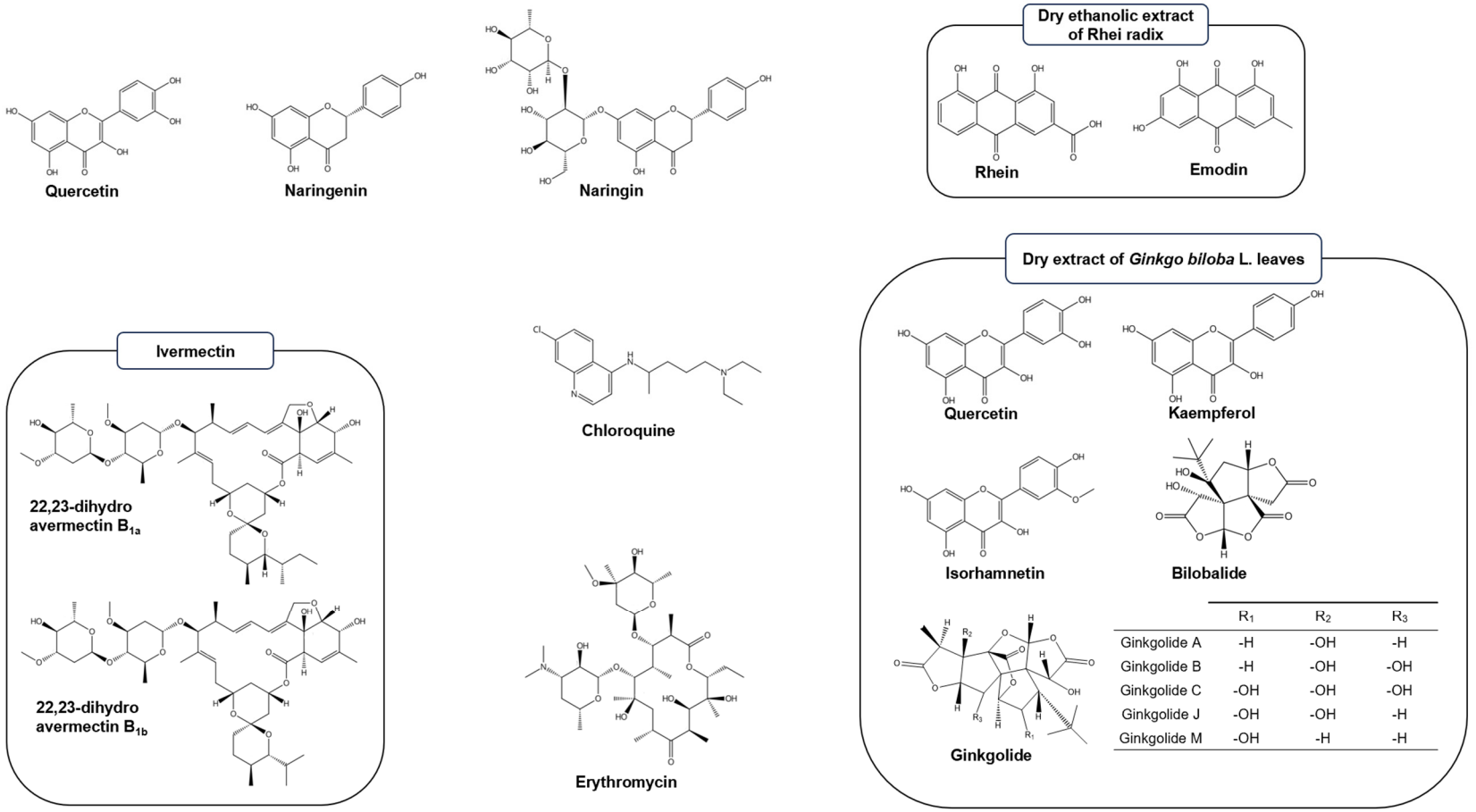

Figure 4. *Cont.*

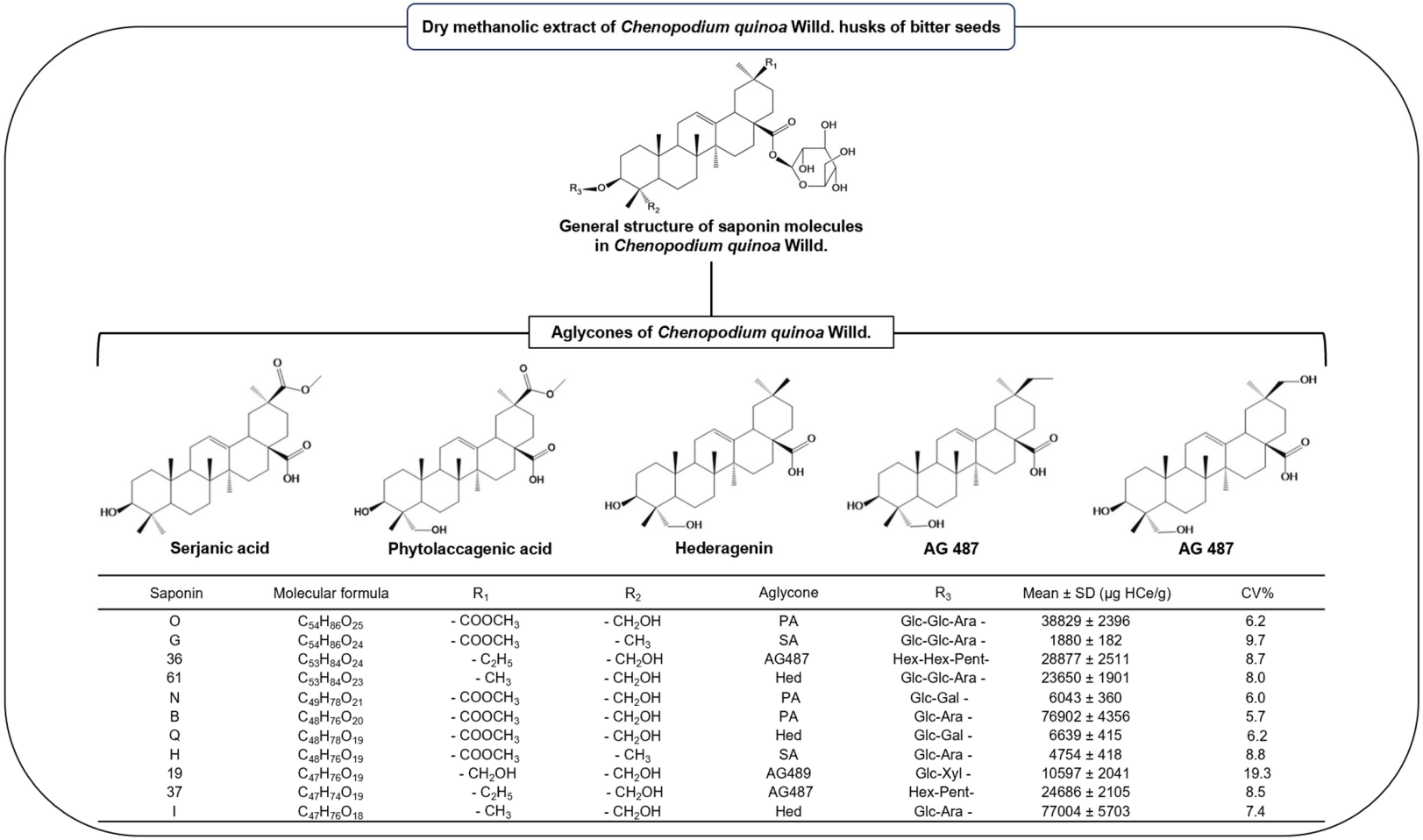

Saponin	Molecular formula	R_1	R_2	Aglycone	R_3	Mean ± SD (µg HCe/g)	CV%
O	$C_{54}H_{86}O_{25}$	- $COOCH_3$	- CH_2OH	PA	Glc-Glc-Ara -	38829 ± 2396	6.2
G	$C_{54}H_{86}O_{24}$	- $COOCH_3$	- CH_3	SA	Glc-Glc-Ara -	1880 ± 182	9.7
36	$C_{53}H_{84}O_{24}$	- C_2H_5	- CH_2OH	AG487	Hex-Hex-Pent-	28877 ± 2511	8.7
61	$C_{53}H_{84}O_{23}$	- CH_3	- CH_2OH	Hed	Glc-Glc-Ara -	23650 ± 1901	8.0
N	$C_{49}H_{78}O_{21}$	- $COOCH_3$	- CH_2OH	PA	Glc-Gal -	6043 ± 360	6.0
B	$C_{48}H_{76}O_{20}$	- $COOCH_3$	- CH_2OH	PA	Glc-Ara -	76902 ± 4356	5.7
Q	$C_{48}H_{78}O_{19}$	- $COOCH_3$	- CH_2OH	Hed	Glc-Gal -	6639 ± 415	6.2
H	$C_{48}H_{76}O_{19}$	- $COOCH_3$	- CH_3	SA	Glc-Ara -	4754 ± 418	8.8
19	$C_{47}H_{76}O_{19}$	- CH_2OH	- CH_2OH	AG489	Glc-Xyl -	10597 ± 2041	19.3
37	$C_{47}H_{74}O_{19}$	- C_2H_5	- CH_2OH	AG487	Hex-Pent-	24686 ± 2105	8.5
I	$C_{47}H_{76}O_{18}$	- CH_3	- CH_2OH	Hed	Glc-Ara -	77004 ± 5703	7.4

Figure 4. Chemical structures of the tested natural products. The figure depicts the major compounds present in tested commercial extracts [91,94–97]; their actual levels were inferred from the analysis certificates issued by the selling companies. For the extracts of Rhei radix and *Ginkgo biloba* L., chemical structures of major compounds are presented to exemplify their complex compositions [96,98]. For Chenopodium quinoa bitter seed husks, compounds were identified and quantified in µg HCe/g (µg hederacoside C equivalents per g of dry weight) by LC-MS-MS according to [91] (mean ± standard deviation; n = 3; limit of detection, 0.83 µg/g; limit of quantification, 2.53 µg/g). PA: phytolaccagenic acid; Hed: hederagenin; SA: serjenic acid; AG489 and AG487 refer to aglycones with a specific m/z; Glc: glucose; Ara: arabinose; Gal: galactose, Xyl: xylose; Hex: hexose; Pent: pentose.

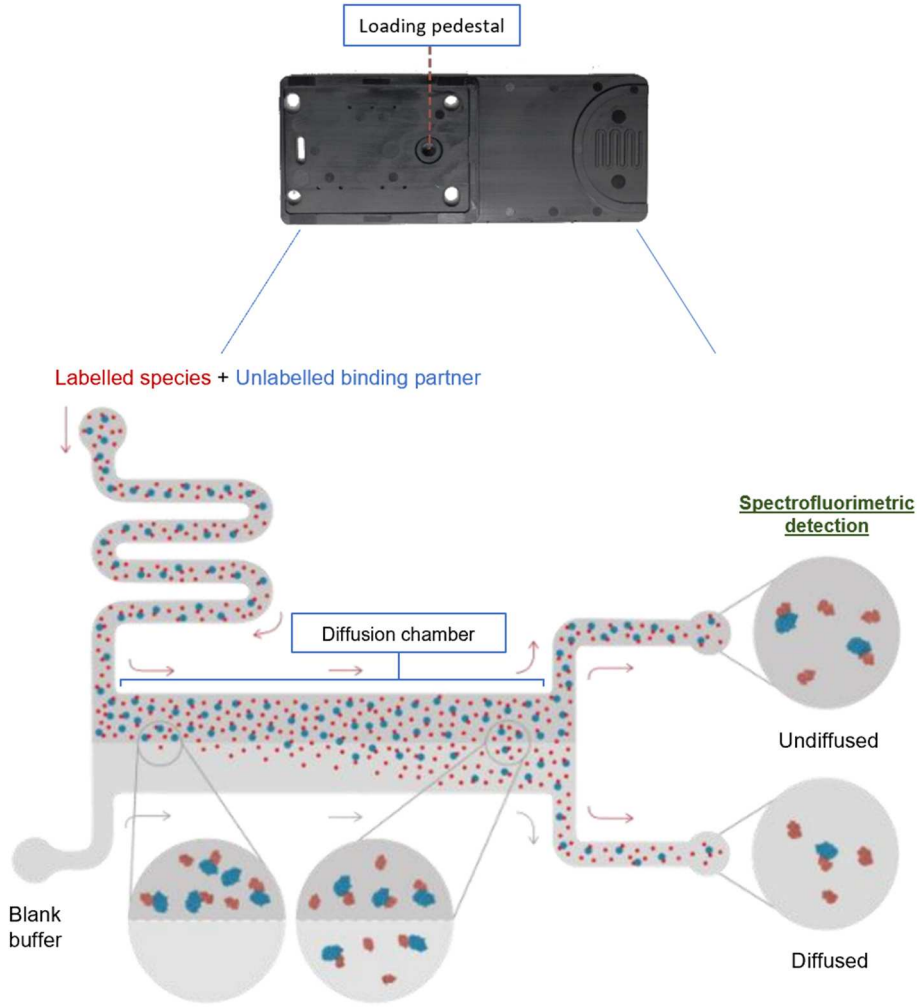

Figure 5. Diagram showing the interior of a microfluidic chip and the travel of the sample after injection on the loading pedestal (adapted from [100,101]).

Measuring R_h at increasing concentrations of the partner species yields a sigmoid curve that corresponds to the saturation of the labeled species by its partner, enabling the determination of the dissociation constant (K_D), either graphically or through a nonlinear least-squares fitting method [16].

Alexa Fluor 647-labeled spike RBD (20 nM) was mixed with unlabeled ACE-2 at increasing concentrations (180 pM to 750 nM) in a solution of DMSO 1% v/v in PBS and incubated at room temperature for 60 min. To assess the formation of complexes via MDS, 5 µL of sample was transferred to a microfluidic chip (100009; Fluidic Analytics, Cambridge, UK), and the hydrodynamic radius of bound proteins (=$R_{h\text{-complex}}$) was determined at $\lambda_{excitation}$ = 630 nm; $\lambda_{emission}$ = 694 nm; and $\lambda_{dichroic}$ = 660 nm with a size range of 0.7 to 5 nm (1 to 200 kDa).

4.4. Modulation of SARS-CoV-2 Spike RBD/ACE2 Affinity by Natural Compounds

To screen potential modulators of SARS-CoV-2 spike RBD-ACE2 receptor binding, the impact of a series of natural compounds on the $R_{h\text{-complex}}$ was measured at defined partner concentrations via MDS. Indeed, focusing on the $R_{h\text{-complex}}$ is better suited to screening than K_D determination, which would require multiple experiments at varying concentrations of both the modulator and the unlabeled partner.

To determine eventual increases or decreases in R_h in the presence of the tested modulators, aliquots of the 2 proteins were mixed with each potential modulator at increasing modulator concentrations to yield protein concentrations of 20 nM (equimolar concentra-

tions near the K_D conditions). The mix of proteins, with and without modulators, was dissolved in a solution of DMSO 1% *v*/*v* in PBS to ensure the solubility of tested natural compounds and extracts; the solutions were incubated at room temperature for 60 min and analyzed via MDS. The spike RBD/ACE2 K_D determined in DMSO 1% *v*/*v* in PBS (19.8 nM) fairly agrees with the K_D determined in PBS (24.2 nM; 95% confidence interval, 10.6 to 48.9 nM; n = 4), indicating no detrimental effect of DMSO on measured values.

4.5. Statistical Analysis of Results

R_h values obtained for each of the tested natural product concentrations were compared to their daily negative control (R_h for the 20 nM equimolar mix of spike RBD and ACE2) by means of one-way ANOVA with post hoc Student's t test (Bonferroni correction) using GraphPad Prism 5 (GraphPad, San Diego, CA, USA) software, and p values < 0.05 were considered significant.

5. Conclusions

The present study investigated the potential of selected natural products to modulate the SARS-CoV-2 spike RBD/ACE2 interaction. Using microfluidic diffusional sizing to measure the hydrodynamic radius of the bound protein complex, the effects of selected natural compounds and extracts were measured, either positive (corresponding to a distension of the complex or to a clustering of natural compounds on proteins) or negative (a collapse or folding of the complex or a partial separation of the two proteins). These data allowed us to highlight several possibly interesting compounds/extracts.

Further investigations of these compounds should include a determination of their effects on K_D and affinity curves, an in silico study of the effective binding sites on the protein complex, and an evaluation of their ability to prevent the cellular entry of SARS-CoV-2 in a relevant cell model.

Notably, a quinoa extract would be interesting to further study for its possible application as an infection-preventing nasal spray; although saponins are known for their sternutatory activity, the low active concentrations needed and the higher polarity and lower amphiphilicity of bisdesmosides may make them low-irritating agents to the nasal mucosa.

Compared to surface plasmon resonance and biolayer interferometry, in which a protein is immobilized on a surface with an often unknown orientation [58–63,65,70], the MDS model has the distinct advantage of working with both protein partners in a free state, with full conformational freedom, which may explain some differences from published K_D and modulatory effects. The development of a memtein model would be an attractive method to study, via MDS, the RBD/ACE2 interaction on an ACE2 protein in its native state, i.e., embedded in its cell membrane [102].

Supplementary Materials: The following supporting information can be downloaded at https://www.mdpi.com/article/10.3390/molecules28248072/s1: Figure S1: Electropherograms of the three samples: Fluorescence-labeled spike RBD ($_{\text{Spike RBD labeled}}$), concentration = 507 nM; ACE2, concentration = 750 nM; PBS-T; Figure S2: Microfluidic diffusional sizing determination of K_D for the spike RBD (20 nM)/ACE2 complex (DMSO, 1% *v*/*v*; room t°). R_h as a function of ACE2 concentration. ACE2, 180 pM–750 nM; spike RBD; 20 nM; mean ± standard deviation (n = 3). All data points were obtained on a single chip. ACE2 concentrations were injected in ascending order, and the remaining traces of the previous sample were carefully removed using a micropipette. Table S1: One chip per data point—Reproducibility; Table S2: One chip to measure several data points; Table S3: Determination of R_h in different conditions—Comparison to theoretical R_h; Table S4: Interday variability of spike RBD-labeled $R_{h\text{-complex}}$; Table S5: Intraday and total variability of the R_h for the spike RBD-labeled/ACE2 complex; Table S6: Within-day variability of spike RBD/ACE2 K_D; Table S7 Quality of adjustment—Determination of the R^2 [103,104].

Author Contributions: Conceptualization, P.D. and A.N.; methodology, J.F.; investigation, J.F. and J.C.; resources, Laboratory of Pharmacognosy and Therapeutic chemistry form UMONS; data curation, J.F.; Visualization, J.Z., writing—original draft preparation, J.C.; writing—review and editing, J.C., A.N., J.F. and P.D. All authors have read and agreed to the published version of the manuscript.

Funding: This work was partly supported by Wallonie-Bruxelles International through the project Wallonie-Bruxelles/China (MOST) "*Anti-inflammatory herbal medicines and their active components to fight the cytokine storm associated with COVID-19 diseases (TCM-Cyt)*". This work was supported by the Fonds pour la Recherche Scientifique FNRS under grant N° CDR J.0058.21 "PlasmLip", which contributed to the acquisition of the fluidity instrument. Veronica Taco is warmly thanked for her analysis of the *Chenopodium quinoa* husk extract and for giving us access to this sample; Veronica Taco is a scholarship holder from the Académie de Recherche et d'Enseignement Supérieur (ARES, Belgium). This work was also supported by the National Key R&D Program of China, 2021YFE0194000.

Institutional Review Board Statement: Not applicable.

Informed Consent Statement: Not applicable.

Data Availability Statement: Data are contained within the article and Supplementary Materials.

Acknowledgments: We thank all three reviewers for their positive comments that allowed us to improve both the introduction and discussion, notably regarding the achievable plasma levels of tested compounds.

Conflicts of Interest: The authors declare no conflict of interest. The funders had no role in the design of the study; in the collection, analyses, or interpretation of data; in the writing of the manuscript; or in the decision to publish the results.

References

1. WHO. World Health Orgarnization. Available online: https://covid19.who.int/table (accessed on 21 October 2023).
2. Bhakti, K. Insuffisance Respiratoire Hypoxémique Aigüe (Syndrome de Détresse Respiratoire Aiguë [SDRA], Ou [ARDS], Acute Respiratory Distress Syndrome). *N. Engl. J. Med.* **2006**, *354*, 2564–2575. [CrossRef]
3. Patel, K.P.; Vunnam, S.R.; Patel, P.A.; Krill, K.L.; Korbitz, P.M.; Gallagher, J.P.; Suh, J.E.; Vunnam, R.R. Transmission of SARS-CoV-2: An update of current literature. *Eur. J. Clin. Microbiol. Infect. Dis.* **2020**, *39*, 2005–2011. [CrossRef] [PubMed]
4. Goel, N.; Jain, A.; Kumari, A. The role of ACE2 receptor and its age related immunity in COVID-19. *Int. J. Pharm. Sci. Rev. Res.* **2020**, *63*, 190–194.
5. Prashantha, C.N.; Gouthami, K.; Lavanya, L.; Bhavanam, S.; Jakhar, A.; Shakthiraju, R.G.; Suraj, V.; Sahana, K.V.; Sujana, H.S.; Guruprasad, N.M.; et al. Molecular screening of antimalarial, antiviral, anti-inflammatory and HIV protease inhibitors against spike glycoprotein of coronavirus. *J. Mol. Graph. Model.* **2021**, *102*, 107769. [CrossRef] [PubMed]
6. Rajah, M.M.; Bernier, A.; Buchrieser, J.; Schwartz, O. The Mechanism and Consequences of SARS-CoV-2 Spike-Mediated Fusion and Syncytia Formation. *J. Mol. Biol.* **2022**, *434*, 167280. [CrossRef]
7. Cai, Y.; Zhang, J.; Xiao, T.; Peng, H.; Sterling, S.M.; Walsh, R.M.; Rawson, S.; Rits-Volloch, S.; Chen, B. Distinct conformational states of SARS-CoV-2 spike protein. *Science* **2020**, *369*, 1586–1592. [CrossRef]
8. Jackson, C.B.; Farzan, M.; Chen, B.; Choe, H. Mechanisms of SARS-CoV-2 entry into cells. *Nat. Rev. Mol. Cell Biol.* **2022**, *23*, 3–20. [CrossRef]
9. Ke, Z.; Oton, J.; Qu, K.; Cortese, M.; Zila, V.; McKeane, L.; Nakane, T.; Zivanov, J.; Neufeldt, C.J.; Cerikan, B.; et al. Structures and distributions of SARS-CoV-2 spike proteins on intact virions. *Nature* **2020**, *588*, 498–502. [CrossRef] [PubMed]
10. Watanabe, Y.; Allen, J.D.; Wrapp, D.; McLellan, J.S.; Crispin, M. Site-specific glycan analysis of the SARS-CoV-2 spike. *Science* **2020**, *369*, 330–333. [CrossRef]
11. Yan, R.; Zhang, Y.; Li, Y.; Ye, F.; Guo, Y.; Xia, L.; Zhong, X.; Chi, X.; Zhou, Q. Structural basis for the different states of the spike protein of SARS-CoV-2 in complex with ACE2. *Cell Res.* **2021**, *31*, 717–719. [CrossRef]
12. Camargo, S.M.R.; Vuille-Dit-Bille, R.N.; Meier, C.F.; Verrey, F. ACE2 and gut amino acid transport. *Clin. Sci.* **2020**, *134*, 2823–2833. [CrossRef]
13. Wiese, O.; Zemlin, A.E.; Pillay, T.S. Molecules in pathogenesis: Angiotensin converting enzyme 2 (ACE2). *J. Clin. Pathol.* **2021**, *74*, 285–290. [CrossRef] [PubMed]
14. Zhang, H.; Penninger, J.M.; Li, Y.; Zhong, N.; Slutsky, A.S. Angiotensin-converting enzyme 2 (ACE2) as a SARS-CoV-2 receptor: Molecular mechanisms and potential therapeutic target. *Intensive Care Med.* **2020**, *46*, 586–590. [CrossRef]
15. Han, P.; Li, L.; Liu, S.; Wang, Q.; Zhang, D.; Xu, Z.; Han, P.; Li, X.; Peng, Q.; Su, C.; et al. Receptor binding and complex structures of human ACE2 to spike RBD from omicron and delta SARS-CoV-2. *Cell* **2022**, *185*, 630–640.e610. [CrossRef] [PubMed]
16. Fiedler, S.; Piziorska, M.A.; Denninger, V.; Morgunov, A.S.; Ilsley, A.; Malik, A.Y.; Schneider, M.M.; Devenish, S.R.A.; Meisl, G.; Kosmoliaptsis, V.; et al. Antibody Affinity Governs the Inhibition of SARS-CoV-2 Spike/ACE2 Binding in Patient Serum. *ACS Infect. Dis.* **2021**, *7*, 2362–2369. [CrossRef] [PubMed]

17. Arosio, P.; Müller, T.; Rajah, L.; Yates, E.V.; Aprile, F.A.; Zhang, Y.; Cohen, S.I.A.; White, D.A.; Herling, T.W.; De Genst, E.J.; et al. Microfluidic diffusion analysis of the sizes and interactions of proteins under native solution conditions. *ACS Nano* **2016**, *10*, 333–341. [CrossRef] [PubMed]
18. Alqathama, A.A.; Ahmad, R.; Alsaedi, R.B.; Alghamdi, R.A.; Abkar, E.H.; Alrehaly, R.H.; Abdalla, A.N. The vital role of animal, marine, and microbial natural products against COVID-19. *Pharm. Biol.* **2022**, *60*, 509–524. [CrossRef]
19. Frediansyah, A.; Sofyantoro, F.; Alhumaid, S.; Al Mutair, A.; Albayat, H.; Altaweil, H.I.; Al-Afghani, H.M.; AlRamadhan, A.A.; AlGhazal, M.R.; Turkistani, S.A.; et al. Microbial natural products with antiviral activities, including anti-SARS-CoV-2: A review. *Molecules* **2022**, *27*, 4305. [CrossRef]
20. Low, Z.; Lani, R.; Tiong, V.; Poh, C.; AbuBakar, S.; Hassandarvish, P. COVID-19 therapeutic potential of natural products. *Int. J. Mol. Sci.* **2023**, *24*, 9589. [CrossRef]
21. Lingwan, M.; Shagun, S.; Pant, Y.; Nanda, R.; Masakapalli, S. Antiviral phytochemicals identified in *Rhododendron arboreum* petals exhibited strong binding to SARS-CoV-2 MPro and Human ACE2 receptor. *Preprints* **2020**, 2020080530. [CrossRef]
22. Liu, W.; Zheng, W.; Cheng, L.; Li, M.; Huang, J.; Bao, S.; Xu, Q.; Ma, Z. Citrus fruits are rich in flavonoids for immunoregulation and potential targeting ACE2. *Nat. Prod. Bioprospecting* **2022**, *12*, 4. [CrossRef] [PubMed]
23. Liu, X.; Raghuvanshi, R.; Ceylan, F.D.; Bolling, B.W. Quercetin and Its Metabolites Inhibit Recombinant Human Angiotensin-Converting Enzyme 2 (ACE2) Activity. *J. Agric. Food Chem.* **2020**, *68*, 13982–13989. [CrossRef]
24. Pan, B.; Fang, S.; Zhang, J.; Pan, Y.; Liu, H.; Wang, Y.; Li, M.; Liu, L. Chinese herbal compounds against SARS-CoV-2: Puerarin and quercetin impair the binding of viral S-protein to ACE2 receptor. *Comput. Struct. Biotechnol. J.* **2020**, *18*, 3518–3527. [CrossRef]
25. Priyandoko, D. Molecular Docking Study of the Potential Relevance of the Natural Compounds Isoflavone and Myricetin to COVID-19. *Int. J. Bioautomation* **2021**, *25*, 271–282. [CrossRef]
26. Shakhsi-Niaei, M.; Soureshjani, E.H.; Babaheydari, A.K. In Silico Comparison of Separate or Combinatorial Effects of Potential Inhibitors of the SARS-CoV-2 Binding Site of ACE2. *Iran J. Public Health* **2021**, *50*, 1028–1036. [CrossRef]
27. Tutunchi, H.; Naeini, F.; Ostadrahimi, A.; Hosseinzadeh-Attar, M.J. Naringenin, a flavanone with antiviral and anti-inflammatory effects: A promising treatment strategy against COVID-19. *Phytother. Res.* **2020**, *30*, 3137–3147. [CrossRef]
28. Abdelli, I.; Hassani, F.; Bekkel Brikci, S.; Ghalem, S. In Silico study the inhibition of angiotensin converting enzyme 2 receptor of COVID-19 by Ammoides verticillata components harvested from Western Algeria. *J. Biomol. Struct. Dyn.* **2020**, *39*, 3263–3276. [CrossRef]
29. Badraoui, R.; Saoudi, M.; Hamadou, W.S.; Elkahoui, S.; Siddiqui, A.J.; Alam, J.M.; Jamal, A.; Adnan, M.; Suliemen, A.M.E.; Alreshidi, M.M.; et al. Antiviral effects of artemisinin and Its derivatives against SARS-CoV-2 main protease: Computational evidences and interactions with ACE2 allelic variants. *Pharmaceuticals* **2022**, *15*, 129. [CrossRef]
30. Chen, Z.; Liu, L.; Gao, C.; Chen, W.; Vong, C.T.; Yao, P.; Yang, Y.; Li, X.; Tang, X.; Wang, S.; et al. Astragali Radix (Huangqi): A promising edible immunomodulatory herbal medicine. *J. Ethnopharmacol.* **2020**, *258*, 112895. [CrossRef] [PubMed]
31. Goswami, T.; Bagchi, B. Molecular Docking study of Receptor Binding Domain of SARS-CoV-2 Spike Glycoprotein with Saikosaponin, a Triterpenoid Natural Product. *ChemRxiv. Camb. Camb. Open Engag.* **2020**. [CrossRef]
32. Rolta, R.; Salaria, D.; Sharma, P.; Sharma, B.; Kumar, V.; Rathi, B.; Verma, M.; Sourirajan, A.; Baumler, D.J.; Dev, K. Phytocompounds of Rheum emodi, Thymus serpyllum, and Artemisia annua Inhibit spike protein of SARS-CoV-2 binding to ACE2 receptor: In silico approach. *Curr. Pharmacol. Rep.* **2021**, *7*, 135–149. [CrossRef] [PubMed]
33. Sinha, S.K.; Shakya, A.; Prasad, S.K.; Singh, S.; Gurav, N.S.; Prasad, R.S.; Gurav, S.S. An in-silico evaluation of different saikosaponins for their potency against SARS-CoV-2 using NSP15 and fusion spike glycoprotein as targets. *J. Biomol. Struct. Dyn.* **2021**, *39*, 3244–3255. [CrossRef] [PubMed]
34. Zeng, M.-S.; Yu, W.-D.; Wang, H.-X.; Liu, J.-Y.; Xu, P.-P. A potential antiviral activity of esculentoside A against binding interactions of SARS-COV-2 spike protein and angiotensin converting enzyme 2 (ACE2). *Int. J. Biol. Macromol.* **2021**, *183*, 2248–2261. [CrossRef] [PubMed]
35. Anwar, F.; Altayb, H.N.; Al-Abbasi, F.A.; Kumar, V.; Kamal, M.A. The computational intervention of macrolide antibiotics in the treatment of COVID-19. *Curr. Pharm. Des.* **2021**, *27*, 1202–1210. [CrossRef] [PubMed]
36. Braz, H.L.B.; Silveira, J.A.d.M.; Marinho, A.D.; de Moraes, M.E.A.; Moraes Filho, M.O.d.; Monteiro, H.S.A.; Jorge, R.J.B. In Silico study of azithromycin, chloroquine and hydroxychloroquine and their potential mechanisms of action against SARS-CoV-2 infection. *Int. J. Antimicrob. Agents* **2020**, *56*, 106119. [CrossRef]
37. Kalhor, H.; Sadeghi, S.; Abolhasani, H.; Kalhor, R.; Rahimi, H. Repurposing of the approved small molecule drugs in order to inhibit SARS-CoV-2 S protein and human ACE2 interaction through virtual screening approaches. *J. Biomol. Struct. Dyn.* **2022**, *40*, 1299–1315. [CrossRef] [PubMed]
38. Lehrer, S.; Rheinstein, P.H. Ivermectin docks to the SARS-CoV-2 spike receptor-binding domain attached to ACE2. *In Vivo* **2020**, *34*, 3023–3026. [CrossRef]
39. Basu, A.; Sarkar, A.; Maulik, U. Molecular docking study of potential phytochemicals and their effects on the complex of SARS-CoV2 spike protein and human ACE2. *Sci. Rep.* **2020**, *10*, 17699. [CrossRef]
40. Du, H.-X.; Zhu, J.-Q.; Chen, J.; Zhou, H.-F.; Yang, J.-H.; Wan, H.-T. Revealing the therapeutic targets and molecular mechanisms of emodin-treated coronavirus disease 2019 via a systematic study of network pharmacology. *Aging* **2021**, *13*, 14571–14589. [CrossRef]

41. Zhan, Y.; Ta, W.; Tang, W.; Hua, R.; Wang, J.; Wang, C.; Lu, W. Potential antiviral activity of isorhamnetin against SARS-CoV-2 spike pseudotyped virus in vitro. *Drug Dev. Res.* **2021**, *82*, 1124–1130. [CrossRef]
42. Gangadevi, S.; Badavath, V.N.; Thakur, A.; Yin, N.; De Jonghe, S.; Acevedo, O.; Jochmans, D.; Leyssen, P.; Wang, K.; Neyts, J.; et al. Kobophenol A Inhibits Binding of Host ACE2 Receptor with Spike RBD Domain of SARS-CoV-2, a Lead Compound for Blocking COVID-19. *J. Phys. Chem. Lett.* **2021**, *12*, 1793–1802. [CrossRef]
43. Perrella, F.; Coppola, F.; Petrone, A.; Platella, C.; Montesarchio, D.; Stringaro, A.; Ravagnan, G.; Fuggetta, M.P.; Rega, N.; Musumeci, D. Interference of Polydatin/Resveratrol in the ACE2:Spike Recognition during COVID-19 Infection. A Focus on Their Potential Mechanism of Action through Computational and Biochemical Assays. *Biomolecules* **2021**, *11*, 1048. [CrossRef]
44. Chen, R.H.; Yang, L.J.; Hamdoun, S.; Chung, S.K.; Lam, C.W.-K.; Zhang, K.X.; Guo, X.; Xia, C.; Law, B.Y.K.; Wong, V.K.W. 1,2,3,4,6-Pentagalloyl Glucose, a RBD-ACE2 Binding Inhibitor to Prevent SARS-CoV-2 Infection. *Front. Pharmacol.* **2021**, *12*, 634176. [CrossRef] [PubMed]
45. Yang, L.J.; Chen, R.H.; Hamdoun, S.; Coghi, P.; Ng, J.P.L.; Zhang, D.W.; Guo, X.; Xia, C.; Law, B.Y.K.; Wong, V.K.W. Corilagin prevents SARS-CoV-2 infection by targeting RBD-ACE2 binding. *Phytomedicine* **2021**, *87*, 153591. [CrossRef] [PubMed]
46. Balkrishna, A.; Pokhrel, S.; Singh, H.; Joshi, M.; Mulay, V.P.; Haldar, S.; Varshney, A. Withanone from Withania somnifera attenuates SARS-CoV-2 RBD and host ACE2 interactions to rescue spike protein induced pathologies in humanized zebrafish model. *Drug Des. Devel. Ther.* **2021**, *15*, 1111–1133. [CrossRef] [PubMed]
47. Caohuy, H.; Eidelman, O.; Chen, T.; Liu, S.; Yang, Q.; Bera, A.; Walton, N.I.; Wang, T.T.; Pollard, H.B. Common cardiac medications potently inhibit ACE2 binding to the SARS-CoV-2 Spike, and block virus penetration and infectivity in human lung cells. *Sci. Rep.* **2021**, *11*, 22195. [CrossRef]
48. Chitsike, L.; Krstenansky, J.; Duerksen-Hughes, P.J. ACE2: S1 RBD interaction-targeted peptides and small molecules as potential COVID-19 therapeutics. *Adv. Pharmacol. Pharm. Sci.* **2021**, *2021*, e1828792. [CrossRef] [PubMed]
49. Clementi, N.; Scagnolari, C.; D'Amore, A.; Palombi, F.; Criscuolo, E.; Frasca, F.; Pierangeli, A.; Mancini, N.; Antonelli, G.; Clementi, M.; et al. Naringenin is a powerful inhibitor of SARS-CoV-2 infection in vitro. *Pharmacol. Res.* **2021**, *163*, 105255. [CrossRef] [PubMed]
50. van Breemen, R.B.; Muchiri, R.N.; Bates, T.A.; Weinstein, J.B.; Leier, H.C.; Farley, S.; Tafesse, F.G. Cannabinoids block cellular entry of SARS-CoV-2 and the emerging variants. *J. Nat. Prod.* **2022**, *85*, 176–184. [CrossRef]
51. Kim, T.; Jeon, S.; Jang, Y.; Gotina, L.; Won, J.; Ju, Y.; Kim, S.; Jang, M.; Won, W.; Park, M.; et al. Platycodin D, a natural component of *Platycodon grandiflorum*, prevents both lysosome- and TMPRSS2-driven SARS-CoV-2 infection by hindering membrane fusion. *Exp. Mol. Med.* **2021**, *53*, 956–972. [CrossRef]
52. Senthil Kumar, K.J.; Gokila Vani, M.; Wang, C.-S.; Chen, C.-C.; Chen, Y.-C.; Lu, L.-P.; Huang, C.-H.; Lai, C.-S.; Wang, S.-Y. Geranium and lemon essential oils and their active compounds downregulate angiotensin-converting enzyme 2 (ACE2), a SARS-CoV-2 spike receptor-binding domain, in epithelial cells. *Plants* **2020**, *9*, 770. [CrossRef]
53. Xu, H.; Liu, B.; Xiao, Z.; Zhou, M.; Ge, L.; Jia, F.; Liu, Y.; Jin, H.; Zhu, X.; Gao, J.; et al. Computational and experimental studies reveal that thymoquinone blocks the entry of coronaviruses into in vitro cells. *Infect. Dis. Ther.* **2021**, *10*, 483–494. [CrossRef] [PubMed]
54. Caly, L.; Druce, J.D.; Catton, M.G.; Jans, D.A.; Wagstaff, K.M. The FDA-approved drug ivermectin inhibits the replication of SARS-CoV-2 in vitro. *Antivir. Res.* **2020**, *178*, 104787. [CrossRef] [PubMed]
55. Große, M.; Ruetalo, N.; Layer, M.; Hu, D.; Businger, R.; Rheber, S.; Setz, C.; Rauch, P.; Auth, J.; Fröba, M.; et al. Quinine Inhibits Infection of Human Cell Lines with SARS-CoV-2. *Viruses* **2021**, *13*, 647. [CrossRef]
56. Wang, N.; Han, S.; Liu, R.; Meng, L.; He, H.; Zhang, Y.; Wang, C.; Lv, Y.; Wang, J.; Li, X.; et al. Chloroquine and hydroxychloroquine as ACE2 blockers to inhibit viropexis of 2019-nCoV Spike pseudotyped virus. *Phytomedicine* **2020**, *79*, 153333. [CrossRef] [PubMed]
57. Ho, T.-Y.; Wu, S.-L.; Chen, J.-C.; Li, C.-C.; Hsiang, C.-Y. Emodin blocks the SARS coronavirus spike protein and angiotensin-converting enzyme 2 interaction. *Antivir. Res.* **2007**, *74*, 92–101. [CrossRef]
58. Lan, J.; Ge, J.; Yu, J.; Shan, S.; Zhou, H.; Fan, S.; Zhang, Q.; Shi, X.; Wang, Q.; Zhang, L.; et al. Structure of the SARS-CoV-2 spike receptor-binding domain bound to the ACE2 receptor. *Nature* **2020**, *581*, 215–220. [CrossRef] [PubMed]
59. Barton, M.I.; MacGowan, S.A.; Kutuzov, M.A.; Dushek, O.; Barton, G.J.; van der Merwe, P.A. Effects of common mutations in the SARS-CoV-2 Spike RBD and its ligand, the human ACE2 receptor on binding affinity and kinetics. *eLife* **2021**, *10*, e70658. [CrossRef] [PubMed]
60. Laffeber, C.; de Koning, K.; Kanaar, R.; Lebbink, J.H.G. Experimental Evidence for Enhanced Receptor Binding by Rapidly Spreading SARS-CoV-2 Variants. *J. Mol. Biol.* **2021**, *433*, 167058. [CrossRef]
61. Liu, H.; Zhang, Q.; Wei, P.; Chen, Z.; Aviszus, K.; Yang, J.; Downing, W.; Jiang, C.; Liang, B.; Reynoso, L.; et al. The basis of a more contagious 501Y.V1 variant of SARS-CoV-2. *Cell Res.* **2021**, *31*, 720–722. [CrossRef]
62. Shang, J.; Ye, G.; Shi, K.; Wan, Y.; Luo, C.; Aihara, H.; Geng, Q.; Auerbach, A.; Li, F. Structural basis of receptor recognition by SARS-CoV-2. *Nature* **2020**, *581*, 221–224. [CrossRef] [PubMed]
63. Supasa, P.; Zhou, D.; Dejnirattisai, W.; Liu, C.; Mentzer, A.J.; Ginn, H.M.; Zhao, Y.; Duyvesteyn, H.M.E.; Nutalai, R.; Tuekprakhon, A.; et al. Reduced neutralization of SARS-CoV-2 B.1.1.7 variant by convalescent and vaccine sera. *Cell* **2021**, *184*, 2201–2211.e7. [CrossRef] [PubMed]
64. Prévost, J.; Richard, J.; Gasser, R.; Ding, S.; Fage, C.; Anand, S.P.; Adam, D.; Vergara, N.G.; Tauzin, A.; Benlarbi, M.; et al. Impact of temperature on the affinity of SARS-CoV-2 Spike for ACE2. *bioRxiv* **2021**, 451812. [CrossRef]

65. Wrapp, D.; Wang, N.; Corbett, K.S.; Goldsmith, J.A.; Hsieh, C.-L.; Abiona, O.; Graham, B.S.; McLellan, J.S. Cryo-EM structure of the 2019-nCoV spike in the prefusion conformation. *Science* **2020**, *367*, 1260–1263. [CrossRef]
66. ReactionBiology. Reaction Biology. Available online: https://www.reactionbiology.com/sites/default/files/Images/Content/Biophysical_Assay/SPR_S%20protein%20ACE2_ReactionBiology_V2.pdf (accessed on 25 October 2023).
67. Allen, J.D.; Watanabe, Y.; Chawla, H.; Newby, M.L.; Crispin, M. Subtle Influence of ACE2 Glycan Processing on SARS-CoV-2 Recognition. *J. Mol. Biol.* **2021**, *433*, 166762. [CrossRef] [PubMed]
68. Kuznetsov, A.; Arukuusk, P.; Härk, H.; Juronen, E.; Langel, Ü.; Ustav, M.; Järv, J. ACE2 peptide fragment interacts with several sites on the SARS-CoV-2 spike protein S1. *bioRxiv* **2020**, 424682. [CrossRef]
69. Walls, A.C.; Park, Y.-J.; Tortorici, M.A.; Wall, A.; McGuire, A.T.; Veesler, D. Structure, Function, and Antigenicity of the SARS-CoV-2 Spike Glycoprotein. *Cell* **2020**, *181*, 281–292.e6. [CrossRef]
70. Zhang, J.; Cai, Y.; Xiao, T.; Lu, J.; Peng, H.; Sterling, S.M.; Walsh, R.M.; Rits-Volloch, S.; Zhu, H.; Woosley, A.N.; et al. Structural impact on SARS-CoV-2 spike protein by D614G substitution. *Science* **2021**, *372*, 525–530. [CrossRef]
71. Ru, J.; Li, P.; Wang, J.; Zhou, W.; Li, B.; Huang, C.; Li, P.; Guo, Z.; Tao, W.; Yang, Y.; et al. TCMSP: A database of systems pharmacology for drug discovery from herbal medicines. *J. Cheminform.* **2014**, *6*, 13. [CrossRef]
72. Smith, M.D.; Smith, J.C. Repurposing Therapeutics for COVID-19: Supercomputer-Based Docking to the SARS-CoV-2 Viral Spike Protein and Viral Spike Protein-Human ACE2 Interface. *ChemRxiv*, 2020; *preprint*.
73. Charles, C.; Nachtergael, A.; Ouedraogo, M.; Belayew, A.; Duez, P. Effects of chemopreventive natural products on non-homologous end-joining DNA double-strand break repair. *Mutat. Res./Genet. Toxicol. Environ. Mutagen.* **2014**, *768*, 33–41. [CrossRef] [PubMed]
74. Rebello, C.J.; Beyl, R.A.; Lertora, J.J.L.; Greenway, F.L.; Ravussin, E.; Ribnicky, D.M.; Poulev, A.; Kennedy, B.J.; Castro, H.F.; Campagna, S.R.; et al. Safety and pharmacokinetics of naringenin: A randomized, controlled, single-ascending-dose clinical trial. *Diabetes Obes. Metab.* **2020**, *22*, 91–98. [CrossRef] [PubMed]
75. Biber, A.; Harmelin, G.; Lev, D.; Ram, L.; Shaham, A.; Nemet, I.; Kliker, L.; Erster, O.; Mandelboim, M.; Schwartz, E. The effect of ivermectin on the viral load and culture viability in early treatment of nonhospitalized patients with mild COVID-19—A double-blind, randomized placebo-controlled trial. *Int. J. Infect. Dis.* **2022**, *122*, 733–740. [CrossRef] [PubMed]
76. González Canga, A.; Sahagún Prieto, A.M.; Diez Liébana, M.J.; Fernández Martínez, N.; Sierra Vega, M.; García Vieitez, J.J. The pharmacokinetics and interactions of ivermectin in humans—A mini-review. *AAPS J.* **2008**, *10*, 42–46. [CrossRef]
77. Lee, J.-H.; Kim, J.M.; Kim, C. Pharmacokinetic analysis of rhein in *Rheum undulatum* L. *J. Ethnopharmacol.* **2003**, *84*, 5–9. [CrossRef] [PubMed]
78. Zhu, W.; Wang, X.-M.; Zhang, L.; Li, X.-Y.; Wang, B.-X. Pharmacokinetic of rhein in healthy male volunteers following oral and retention enema administration of rhubarb extract: A single dose study. *Am. J. Chin. Med.* **2005**, *33*, 839–850. [CrossRef] [PubMed]
79. Mieres-Castro, D.; Mora-Poblete, F. Saponins: Research Progress and Their Potential Role in the Post-COVID-19 Pandemic Era. *Pharmaceutics* **2023**, *15*, 348. [CrossRef]
80. Ogunyemi, O.M.; Gyebi, G.A.; Ibrahim, I.M.; Olaiya, C.O.; Ocheje, J.O.; Fabusiwa, M.M.; Adebayo, J.O. Dietary stigmastane-type saponins as promising dual-target directed inhibitors of SARS-CoV-2 proteases: A structure-based screening. *RSC Adv.* **2021**, *11*, 33380–33398. [CrossRef]
81. Rehan, M.; Shafiullah. Medicinal plant-based saponins targeting COVID-19 M^{pro} in silico. *Tradit Med. Res.* **2021**, *6*, 21–30. [CrossRef]
82. Falade, V.A.; Adelusi, T.I.; Adedotun, I.O.; Abdul-Hammed, M.; Lawal, T.A.; Agboluaje, S.A. In Silico investigation of saponins and tannins as potential inhibitors of SARS-CoV-2 main protease (M^{pro}). *Silico Pharmacol.* **2021**, *9*, 9. [CrossRef]
83. Chen, H.; Du, Q. Potential Natural Compounds for Preventing SARS-CoV-2 (2019-nCoV) Infection. *Preprints* **2020**. [CrossRef]
84. Yan, Y.; Shen, X.; Cao, Y.; Zhang, J.; Wang, Y.; Cheng, Y. Discovery of Anti-2019-nCoV Agents from Chinese Patent Drugs via Docking Screening. *Preprints* **2020**, 2020020254. [CrossRef]
85. Cheng, P.W.; Ng, L.T.; Chiang, L.C.; Lin, C.C. Antiviral effects of saikosaponins on human coronavirus 229E in vitro. *Clin. Exp. Pharmacol. Physiol.* **2006**, *33*, 612–616. [CrossRef] [PubMed]
86. Cinatl, J.; Morgenstern, B.; Bauer, G.; Chandra, P.; Rabenau, H.; Doerr, H.W. Glycyrrhizin, an active component of liquorice roots, and replication of SARS-associated coronavirus. *Lancet* **2003**, *361*, 2045–2046. [CrossRef] [PubMed]
87. Chen, F.; Chan, K.H.; Jiang, Y.; Kao, R.Y.; Lu, H.T.; Fan, K.W.; Cheng, V.C.; Tsui, W.H.; Hung, I.F.; Lee, T.S.; et al. In Vitro susceptibility of 10 clinical isolates of SARS coronavirus to selected antiviral compounds. *J. Clin. Virol.* **2004**, *31*, 69–75. [CrossRef] [PubMed]
88. Hoever, G.; Baltina, L.; Michaelis, M.; Kondratenko, R.; Baltina, L.; Tolstikov, G.A.; Doerr, H.W.; Cinatl, J., Jr. Antiviral activity of glycyrrhizic acid derivatives against SARS-coronavirus. *J. Med. Chem.* **2005**, *48*, 1256–1259. [CrossRef]
89. Wu, C.Y.; Jan, J.T.; Ma, S.H.; Kuo, C.J.; Juan, H.F.; Cheng, Y.S.; Hsu, H.H.; Huang, H.C.; Wu, D.; Brik, A.; et al. Small molecules targeting severe acute respiratory syndrome human coronavirus. *Proc. Natl. Acad. Sci. USA* **2004**, *101*, 10012–10017. [CrossRef]
90. Yu, K.; Chen, F.; Li, C. Absorption, disposition, and pharmacokinetics of saponins from chinese medicinal herbs: What do we know and what do we need to know more? *Curr. Drug Metab.* **2012**, *13*, 577–598. [CrossRef] [PubMed]
91. Taco, V.; Savarino, P.; Benali, S.; Villacrés, E.; Raquez, J.-M.; Gerbaux, P.; Duez, P.; Nachtergael, A. Deep eutectic solvents for the extraction and stabilization of Ecuadorian quinoa (*Chenopodium quinoa* Willd.) saponins. *J. Clean. Prod.* **2022**, *363*, 132609. [CrossRef]

92. Sha, A.; Liu, Y.; Hao, H. Current state-of-the-art and potential future therapeutic drugs against COVID-19. *Front. Cell Dev. Biol.* **2023**, *11*, 1238027. [CrossRef]
93. Wu, A.; Shi, K.; Wang, J.; Zhang, R.; Wang, Y. Targeting SARS-CoV-2 entry processes: The promising potential and future of host-targeted small-molecule inhibitors. *Eur. J. Med. Chem.* **2024**, *263*, 115923. [CrossRef]
94. Lin, Y.-L.; Wu, C.-F.; Huang, Y.-T. Phenols from the roots of Rheum palmatum attenuate chemotaxis in rat hepatic stellate cells. *Planta Med.* **2008**, *74*, 1246–1252. [CrossRef] [PubMed]
95. Sigma-Aldrich. Available online: https://www.sigmaaldrich.com/certificates/Graphics/COfAInfo/fluka/pdf/rtc/PHR1380_LRAC6468.pdf (accessed on 18 November 2023).
96. van Beek, T.A.; Montoro, P. Chemical analysis and quality control of Ginkgo biloba leaves, extracts, and phytopharmaceuticals. *J. Chromatogr. A* **2009**, *1216*, 2002–2032. [CrossRef] [PubMed]
97. Wang, C.-C.; Huang, Y.-J.; Chen, L.-G.; Lee, L.-T.; Yang, L.-L. Inducible nitric oxide synthase inhibitors of chinese herbs III. Rheum palmatum. *Planta Med.* **2002**, *68*, 869–874. [CrossRef] [PubMed]
98. EMA. *Assessment Report on Rheum palmatum L. and Rheum Officinale Baillon, Radix*; HMPC—European Medicines Agency: Amsterdam The Netherlands, 2020.
99. Fluidic Analytics. Available online: https://www.fluidic.com/ (accessed on 21 October 2023).
100. Fluidic Analytics. *User Guide for Fluidity™ One-M IFU-0011 v4*; Fluidic Analytics: Cambridge, UK, 2022; p. 12.
101. Fluidic Analytics. *User Manual for Fluidity One-W and Fluidity One-W Serum IFU-0007v8*; Fluidic Analytics: Cambridge, UK, 2021; p. 9.
102. Overduin, M.; Esmaili, M. Memtein: The fundamental unit of membrane-protein structure and function. *Chem. Phys. Lipids* **2019**, *218*, 73–84. [CrossRef]
103. Fluidic Analytics. Available online: https://www.fluidic.com/resources/hydrodynamicradius-and-protein-weight/ (accessed on 9 April 2022).
104. Fluidic Analytics. Available online: https://www.fluidic.com/calculators-page/ (accessed on 23 October 2023).